Effect of boundary conditions on diffusion in two-dimensional granular gases

C. Henrique,[1] G. Batrouni,[2] and D. Bideau[1]
[1]*Groupe Matière Condensée et Matériaux Université de Rennes I, Bâtiment 11A, 263, Avenue du Général Leclerc CS 74205, 35042 Rennes Cedex, France*
[2]*Institut Non-Linéaire de Nice, Université de Nice-Sophia Antipolis, 1361 Route des Lucioles, 06560 Valbonne, France*
(Received 22 March 2000; published 18 December 2000)

We analyze the influence of boundary conditions on numerical simulations of the diffusive properties of a two-dimensional granular gas. We show in particular that periodic boundary conditions introduce unphysical correlations in time that cause the coefficient of diffusion to be strongly dependent on the system size. On the other hand, in large enough systems with hard walls at the boundaries, diffusion is found to be independent of the system size. We compare the results obtained in this case with Langevin theory for an elastic gas. Good agreement is found. We then calculate the relaxation time and the influence of the mass for a particle of radius R_s in a sea of particles of radius R_b. As granular gases are dissipative, we also study the influence of an external random force on the diffusion process in a forced dissipative system. In particular, we analyze differences in the mean-square velocity and displacement between the elastic and inelastic cases.

DOI: 10.1103/PhysRevE.63.011301 PACS number(s): 45.05.+x, 46.55.+d, 46.90.+s

I. INTRODUCTION

The interactions among grains and between grains and the boundaries influence profoundly the macroscopic behavior of granular systems. To study such complex many-body systems, numerical simulations are frequently used where one of the most important ingredients are the collision laws introduced to treat interactions [1]. For dilute assemblies of grains one can use molecular-dynamics algorithms, where periodic boundary conditions are usually used. If the system is initially in a square box, a particle going out on the left re-enters the system on the right. We will show below that this kind of boundary condition modifies the general dynamics of the grains and introduces large correlations in time. This changes the diffusive behavior of the grains. In this paper, we propose an alternative approach to calculate numerically the coefficient of diffusion, accurately and with only very small finite-size effects. To validate our methods, we compare our results for an elastic gas with the Langevin theory.

As granular gases are dissipative it is necessary to feed energy into the system to keep the particles agitated. To thermalize the system, we choose a random acceleration added to each grain at regular time step intervals dt. Our final goal in this paper is to study the dependence of the dynamic properties of the granular gas on the mode used to force the system. This work is a first step towards understanding the diffusion process in a binary system composed of two grain sizes. The system considered here is composed of one particle *s*, of radius R_s in a sea of particles of radius R_b. The particles are spheres constrained to move in a plane and which interact along their equators so that the system is two-dimensional (2D). The system considered here is dilute with a packing fraction of 30%. The simulations are done with the molecular-dynamics algorithms (*time step driven* [2] and *event driven* [3]).

To characterize the diffusive behavior, we focus on the mean-square displacement of the *s* particle. It is well known that for a two-dimensional (2D) gas, the integral of the autocorrelation function does not converge [4]. This means that the mean-square displacement does not vary linearly with time. Therefore, strictly speaking, we cannot define a diffusion coefficient in 2D. However, we show that in a limited range of time, in the stationary state, the mean-square displacement can be approximated by the linear function:

$$\langle[\vec{r}(t+t_0)-\vec{r}(t_0)]^2\rangle \propto 4Dt, \tag{1.1}$$

where D can be interpreted as a diffusion coefficient. All quantities are expressed in arbitrary units.

II. CHOICE OF BOUNDARY CONDITIONS

In this section we show that periodic boundary conditions introduce strong correlations and therefore alter the diffusion process.

A. Periodic boundary conditions

Consistent with common practice, we have used periodic boundary conditions to simulate a system of identical spheres $R_s=R_b=0.5$. Initially the particles are placed randomly in a square box of length L. The number of particles is calculated for each system depending on L, R_s, and the packing fraction. Periodic boundary conditions are applied in both directions. In this case, for elastic or forced gases (Sec. IV), we have observed a strong dependence of D (or of the mean-square displacement) on the system size.

In Fig. 1, we have plotted the mean-square displacement $\langle[\vec{r}(t+t_0)-\vec{r}(t_0)]^2\rangle$ [Fig. 1(a)] and $\int C(t)dt$ [Fig. 1(b)], both calculated in the stationary state, as function of t. $C(t)$ is the normalized autocorrelation function:

$$C(t)=\frac{\langle\vec{v}(t_0+t)\vec{v}(t_0)\rangle-\langle\vec{v}(t_0)\rangle^2}{\langle\vec{v}(t_0)^2\rangle-\langle\vec{v}(t_0)\rangle^2}. \tag{2.1}$$

First, we note that the mean-square displacement, at large time, varies linearly with time as expected but the slope of the curve, i.e., the diffusion coefficient, increases with system size. We show, in the inset to Fig. 1(a), that this depen-

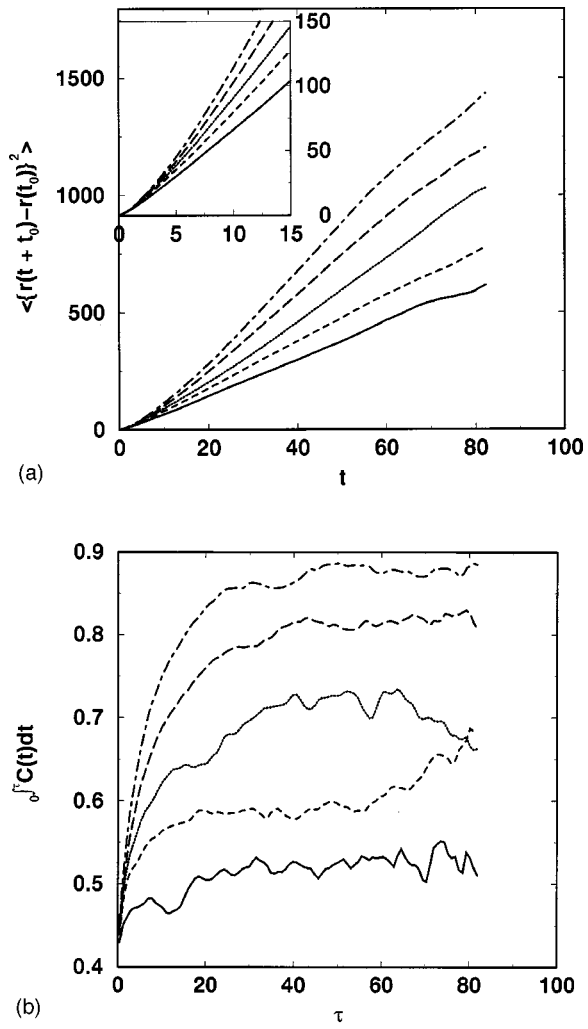

FIG. 1. Dependence of the mean-square displacement on the system size. (a) $\langle[\vec{r}(t+t_0)-\vec{r}(t_0)]^2\rangle$ as a function of t. From bottom to top the system size is 20, 40, 30, 50, and 60. (b) Integral of $C(t)$ as a function of t for the same system. From bottom to top the system size is 20, 40, 30, 50, and 60, respectively.

dence on L appears already at short time, when $\langle[r^2(t+t_0)-\vec{r}(t_0)]^2\rangle \ll L^2$. This feature can be also observed in $\int_0^{t\sim\infty} C(t)dt$, which is proportional to the diffusion coefficient. Similarly, we observe that the relaxation time τ_r [i.e., $C(\tau_r)\simeq 0$] increases with size. In summary, the bigger the system is, the longer the characteristic time τ_r and the larger the diffusion coefficient D are. We recall that such dependence has been observed by Alder *et al.* [5]. They proposed the following law for the dependence of D on the number of particles, N:

$$D(N)=D(\infty)(1-2/N). \tag{2.2}$$

However, their numerical simulations do not support this conjecture [6] since they fail to observe any saturation of D for large systems. In addition, they found strong correlations in the velocity field characterized by the presence of vortex flow pattern at the microscopic scale. Our results confirm the

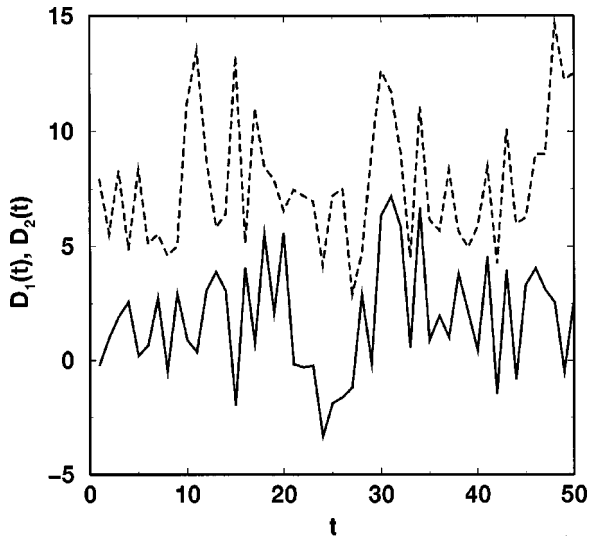

FIG. 2. D_1 and D_2 vs time for a typical monodisperse case with periodic boundaries.

lack of convergence for D with system size. In addition, this variation of D with L is also observed in the case of inelastic collisions.

Another important remark is in order. If the system size is, for example, 60 (with 1400 particles of radius $R=0.5$), the characteristic time τ_r is found to be around 20, which represents about 200 collisions for a particle. This means that a particle needs to undergo 200 collisions to lose completely the memory of its past. According to the Boltzmann theory this time should be limited to only a few collisions. Therefore we cannot accept this result as a valid macroscopic description of a gas. It is worth noting that the same results are found for both, the time step driven and the event driven algorithms.

We now discuss some points helpful for understanding the problem. Initially, each particle has a random velocity drawn from a Maxwellian distribution. We shift the linear and angular momenta so that the system has zero center-of-mass momentum and zero angular momentum relative to the center-of-mass. We find, however, that, although the system keeps its center-of-mass at rest throughout the simulation, the system is no longer isotropic, its moment of inertia becoming that of an ellipsoid. Let $I(t)$ be the inertia matrix of the system. Its two eigenvalues λ_n and λ_p are related via

$$\lambda_n+\lambda_p=m\sum_{k=1}^{N} r_k^2(t), \tag{2.3}$$

where the sum is over all N particles each of mass m. Following λ_n and λ_p in time shows that the system takes an ellipsoidal form ($\lambda_n<\lambda_p$). We have found, as well, an anisotropy in the diffusion tensor $\hat{D}(t)$ defined from $I(t)$ as

$$\hat{D}(t)=\frac{1}{Nm}\frac{I(t+\delta t)-I(t)}{\delta t}. \tag{2.4}$$

As example we show, in Fig. 2 the two eigenvalues D_1 and D_2 of $\hat{D}$ as functions of t for a particular periodic system.

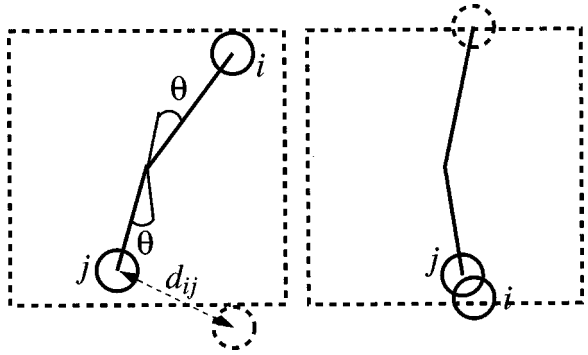

FIG. 3. Illustration of the nonconservation of the distance between two particles.

Clearly, D_1 and D_2 are very different for all t. For all systems we studied, we found two different diffusion coefficients, which depend strongly the system size. We were not able to find how these values scale with L.

In addition, we have found that as the system evolves it will start to rotate even though the initial condition is rotation free. This rotation is put in evidence by calculating the two eigenvectors $\vec{u}_n$ and $\vec{u}_p$ of $I(t)$. These two (perpendicular) vectors rotate in space and, most importantly, they keep the same direction of rotation for a long time ($\sim \tau_r$). We suspect that this rotation induces an anomalous temporal correlation of velocities. One should point out that this rotation phenomenon seems similar to that observed by Alder *et al.* in their simulations with similar periodic boundary conditions.

The reason the system starts to rotate is as follows: The square geometry of the system does not permit the conservation of distances between two particles when the system is rotating. In Fig. 3 we show that after a rotation of θ the distance d_{ij} between particles i and j can be drastically changed by the rotation if one of them goes through the boundary. Because the distance between particles is not conserved by rotation, the interaction potential used in the algorithm, which depends only on the relative positions of particles d_{ij}, is itself not invariant under rotation and so the angular momentum of the system is not conserved. Effectively the total angular momentum is fluctuating as one can see in Fig. 4. Every time a particle goes through the boundary, its angular momentum, l_z^i, changes sign. Consequently, the change in angular momentum is $\Delta L_z = -2l_z^i$. ΔL_z is always proportional to L (the system size) and the total number of particles N, is proportional to L^2. However it appears that the fluctuations of L_z get bigger with system size (see Fig. 4).

The use of periodic boundary conditions amounts to replicating the system on a square lattice. There are, therefore, several identical systems that interact through the boundaries. The rotation observed in our system is then extended to all these systems and can create some shear stress, due to frustration of rotation, between neighboring systems.

These boundary conditions can have other consequences on the dynamics of granular systems. For example, during the simulation of a cooling state the system evolves towards clusters [7] whose orientation depends on the type of boundary conditions [8]. In other similar simulations [9] it was shown that there exist large spatial correlations between particles where the velocities stay correlated over a distance of about $L/2$.

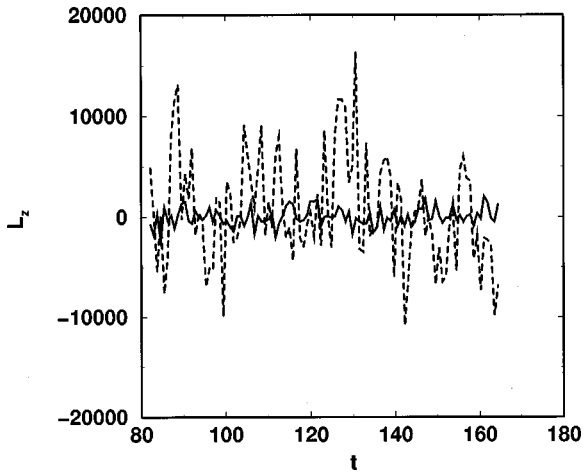

FIG. 4. Total angular momentum $L_z(t)$ vs t for two system lengths and the same particle density. (Full line): $L=20$, (dashed line): $L=50$.

B. Reflecting boundaries

In the case of reflecting boundaries the system is rotationally invariant leading to better behavior of the mean-square displacement. However, in this case, the mean-square displacement is limited at long time by the system size. To circumvent this problem, we proceed as follows. The test particle s is initially put at the center of system at $t=0$. The evolution of the position and velocity of this test particle are then followed until it reaches the boundary of the system in time t_w. We then repeat this many times collecting statistics for many test particles with different initial velocities.

The mean-square displacement is calculated over 500 such trajectories and limited to time smaller than the smallest t_w. In this case, as one can see in Fig. 5, there is no dependence of the mean-square displacement on the system size. Therefore, we can now trust the results of our numerical simulations.

We recall that the integral of the velocity correlation function does not converge in 2D. However, in a limited range of time (see Fig. 5), the quantity $\langle[\vec{r}(t+t_0)-\vec{r}(t_0)]^2\rangle$ can be approximated by a straight line and D calculated according to Eq. (1.1). Therefore, the estimate of D with this method is an approximation.

III. DIFFUSION IN AN ELASTIC GAS

We first validate our algorithm using reflecting boundaries for an elastic gas (i.e., where the collision between particles are elastic). Then, we compare the numerical results with those given by the Langevin equation. Indeed, near equilibrium, the dynamics of s can be described approximately, by a Langevin equation:

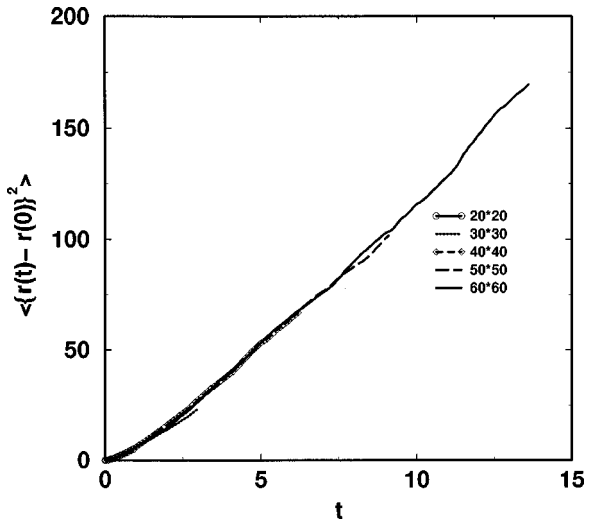

FIG. 5. $\langle[\vec{r}(t)-\vec{r}(0)]^2\rangle$ as function of t using reflecting boundaries. Superposed (as in Fig. 1) are the results for system sizes: 20, 30, 40, 50, and 60.

$$\frac{dv_i(t)}{dt}=-\gamma v_i(t)+\Gamma_i(t),$$
$$\langle\Gamma_i(t)\Gamma_j(t')\rangle=q\,\delta_{i,j}\delta(t-t'), \tag{3.1}$$

where i denotes the two direction x and y. Integrating Eq. (3.1), the dependence of the mean-square velocity on time is simply given by

$$v^2(t)=v^2(0)e^{-2\gamma t}+\frac{q}{\gamma}(1-e^{-2\gamma t}). \tag{3.2}$$

In this paper v denotes the instantaneous velocity of one particle and v^2 the mean-square velocity averaged over the different s trajectories. We can rewrite Eq. (3.2) using the mean square velocity in the equilibrium state $v^2(\infty)=q/\gamma$:

$$v^2(t)=v^2(\infty)+[v^2(0)-v^2(\infty)]e^{-2\gamma t}, \tag{3.3}$$

where $1/\gamma$ corresponds to the relaxation time.

For example, if $R_s \gg R_b$ or, equivalently, $m_s \gg m_b$ ($m_{s,b}$ is the mass of the particle of radius $R_{s,b}$) (see Fig. 6), $1/\gamma$ is very large: the collision of s with a light particle b will not affect strongly the velocity of s. So a great number of collisions is needed before s reaches its equilibrium state. Knowing the total kinetic energy of the system $E_k^{\rm tot}$ (which is given by the initial velocity of each particle), we can easily calculate the square velocity in the equilibrium state $v^2(\infty)=q/\gamma$ (using the Boltzmann distribution law for elastic gases). Using the simulations to calculate $v^2(t)$ for the s particles for initial conditions which are very different from the stationary state, i.e., $v^2(0)\neq v^2(\infty)$ and comparing with Eq. (3.3), we obtain the relaxation time for a big (heavy) particle (Fig. 7). Note that we are looking for agreement near the equilibrium state, where Eq. (3.1) is valid. Indeed the dissipation term γ must depend on both velocities v_s^2 and v_b^2, as we will show.

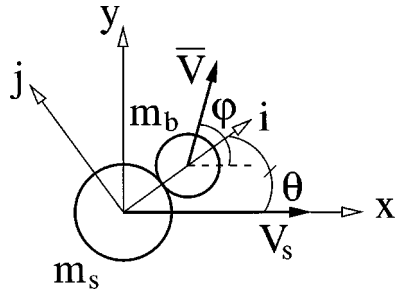

FIG. 6. A particle of mass m_s colliding with a particle of mass m_b: definition of the angles θ and φ.

Equation (3.1) also gives the mean-square displacement as a function of time,

$$\langle[\vec{r}(t)-\vec{r}(0)]^2\rangle=\left(v_0^2-\frac{q}{\gamma}\right)\times\frac{(1-e^{-\gamma t})^2}{\gamma^2}+\frac{2q}{\gamma^2}t-\frac{2q}{\gamma^3}(1-e^{-\gamma t}). \tag{3.4}$$

Comparing Eq. (3.4) and Eq. (1.1) at large time, the coefficient of diffusion is seen to be $D=v^2(\infty)/2\gamma$. In Fig. 7, we compare the theoretical mean square displacement, Eq. (3.4), with the numerical one, obtained for the case $R_s=3R_b$. Note that in Eq. (3.4) all the parameters are known. Clearly, the agreement is very good. This confirms that even for a large test particle, the motion is well described by the simple Langevin equation. This observation, while reasonable, is not trivial since the limited size of our system and the radius of the particles are comparable to the mean-free-path.

We can now present a theoretical calculation of γ, which describes dissipation in the Langevin equation for all pairs (R_s,R_b). This will allow us to compare the theoretical values with the numerical ones as a function of R_s.

The value of γ depends on both velocities, v_s and v_b. To estimate theoretically the value of γ, we consider the deviation, due to a collision, of the particle s moving at v_s in the x direction. The dissipative term $-\gamma\vec{v}_i$ appearing in Eq. (3.1), in the x direction, can therefore be formally written as

$$-\gamma v_s=\left\langle\frac{\vec{v}_s'\cdot\vec{x}-v_s}{v_s}\right\rangle\omega_c v_s, \tag{3.5}$$

where $\vec{v}_s'$ is the velocity after the collision and ω_c is the rate of collision. The symbol $\langle\ \rangle$ in Eq. (3.5) corresponds to the average over all collisions between the s particle and the b particles. To calculate the different terms, we proceed as follows. We consider the collision of s with a particle b moving at a velocity $\vec{v}_b$. The collision is characterized by two angles: θ, the angle between $(\vec{r}_s-\vec{r}_b)$ and the x axis, and φ the angle between $\vec{v}_b$ and the x axis. Then, for such a collision, illustrated in Fig. 6, we can calculate theoretically $\vec{v}_s'(\theta,\varphi)$, the final velocity of the s particle.

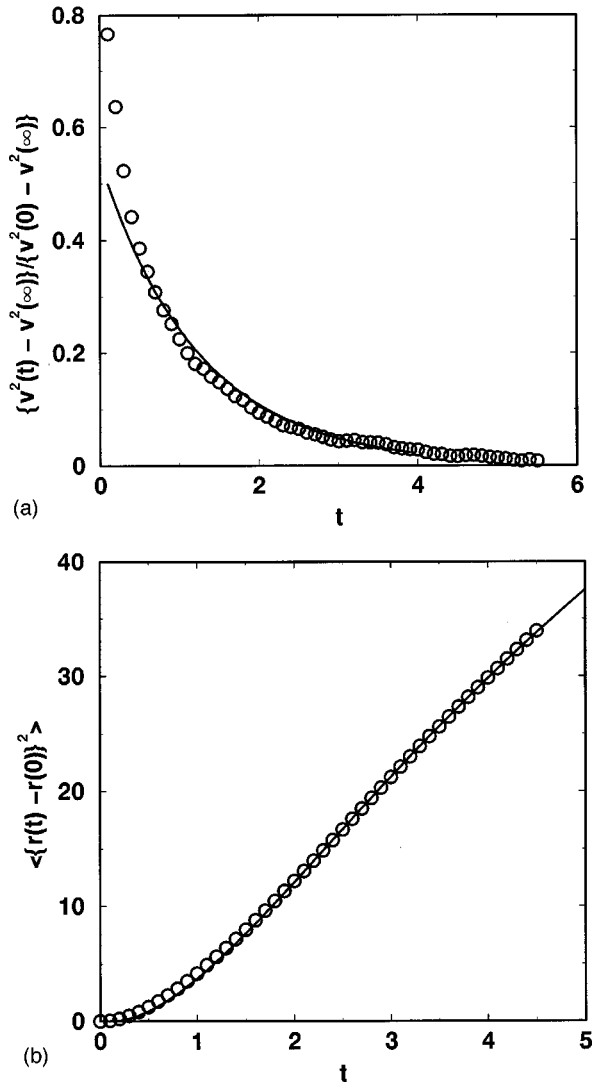

FIG. 7. Comparison between numerical results and Langevin approximation. $R_s=1.5$ and $R_b=0.5$. (a) Dependence of the mean-squared velocity on t; ○: numerical result, full line: fit using $e^{-2\gamma t}$ according to Eq. (3.2). (b) The mean-squared displacement, ○: numerical result, full line: Theoretical prediction according to Eq. (3.3) using for γ the value obtained from (a).

For elastic collisions, the projection of $\vec{v}_s'(\theta,\varphi)$ on the $\vec{x}$ direction is given by

$$\vec{v}_s'(\theta,\varphi)\cdot\vec{x}=\frac{m_s-m_b}{m_s+m_b}v_s\cos^2(\theta)+\frac{2m_b}{m_s+m_b}v_b\cos(\theta)\cos(\theta-\varphi)+v_s\sin^2(\theta), \tag{3.6}$$

with the collision taking place only if

$$v_s\cos(\theta)-v_b\cos(\theta-\varphi)>0. \tag{3.7}$$

Integrating over φ and taking into account Eq. (3.7) we can write

$$\langle\vec{v}_s'(\theta)\cdot\vec{x}\rangle_\varphi=\frac{\int_0^{2\pi}\mathcal{E}_v[v_s\cos(\theta)-v_b\cos(\theta-\varphi)]\vec{v}_s'(\theta,\varphi)\vec{x}\,d\varphi}{\int_0^{2\pi}\mathcal{E}_v[v_s\cos(\theta)-v_b\cos(\theta-\varphi)]}, \tag{3.8}$$

where $\mathcal{E}_v$ is the Heavyside function. We found for Eq. (3.8) two solutions depending on the velocities. If $v_s<v_b$, we have

$$\langle\vec{v}_s'(\theta)\cdot\vec{x}\rangle_\varphi=\frac{m_s-m_b}{m_s+m_b}v_s\cos^2(\theta)+v_s\sin^2(\theta)-\frac{2m_bv_b\cos(\theta)\sin(\theta_p)}{(\pi-\theta_p)(m_s+m_b)} \tag{3.9}$$

for all θ $(0\leqslant\theta\leqslant\pi)$ and with $\theta_p=\cos^{-1}[v_s\cos(\theta)/v_b]$. For the second case, $v_s>v_b$, there is a critical angle, $\theta_c=\cos^{-1}(v_b/v_s)$, such that for $\pi-\theta_c<\theta\leqslant\pi+\theta_c$ the collision does not take place. In this case the solution of Eq. (3.8) is

$$\langle\vec{v}_s'(\theta)\cdot\vec{x}\rangle_\varphi=\frac{m_s-m_b}{m_s+m_b}v_s\cos^2(\theta)+v_s\sin^2(\theta)\quad\text{for}\quad 0\leqslant\theta<\theta_c,$$

$$\langle\vec{v}_s'(\theta)\cdot\vec{x}\rangle_\varphi=\frac{m_s-m_b}{m_s+m_b}v_s\cos^2(\theta)+v_s\sin^2(\theta)-\frac{2m_bv_b\cos(\theta)\sin(\theta_p)}{(\pi-\theta_p)(m_s+m_b)}\quad\text{for}\quad\theta_c\leqslant\theta\leqslant\pi-\theta_c. \tag{3.10}$$

We call $\nu(\theta)$ the mean relative loss of velocity,

$$\nu(\theta)=\frac{\langle\vec{v}_s'(\theta)\cdot\vec{x}\rangle_\varphi-v_s}{v_s},$$

averaging only over the angle φ. In Fig. 8 we show $\nu(\theta)$ for the particular case $R_s=0.25$ and $R_b=0.5$, which means that $v_s>v_b$. Note that in our calculation, the terms v_s and v_b correspond to the averaged values with respect to the appropriate Maxwellian distribution. To obtain the mean value $\tilde{\nu}$ of ν, we average by integrating numerically over θ.

To conclude the calculation of the dissipative term $-\gamma v_s$, we have to estimate, using Eq. (3.5), the collision frequency that also depends on the velocities of the two particles. A similar calculation of ν can be done [10]. In the stationary state, where v_s^2 and v_b^2 are constant and the distributions of the velocities are Maxwellian, one can use [11]

$$\omega_c=\chi\sqrt{\pi}(R_s+R_b)d\sqrt{v_s^2+v_b^2}, \tag{3.11}$$

where d is the density of b particles and χ is a correction factor, which corresponds to the local radial distribution around the s particle.

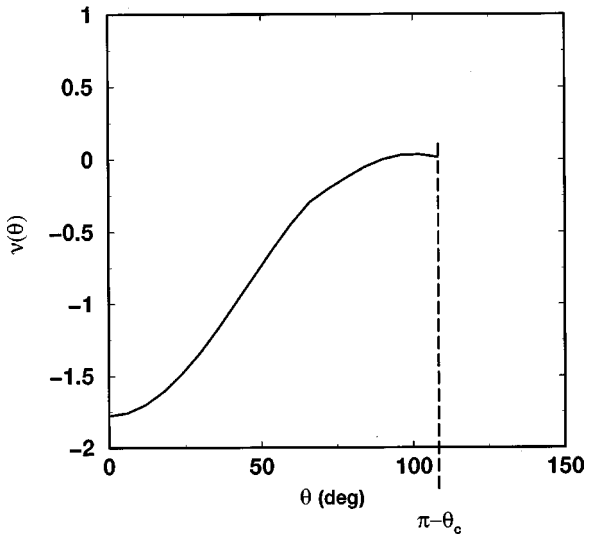

FIG. 8. $\nu(\theta)$, the mean relative loss of energy per collision in the θ direction, for $R_s=0.25$, $R_b=0.5$, and $v_b^2=25$.

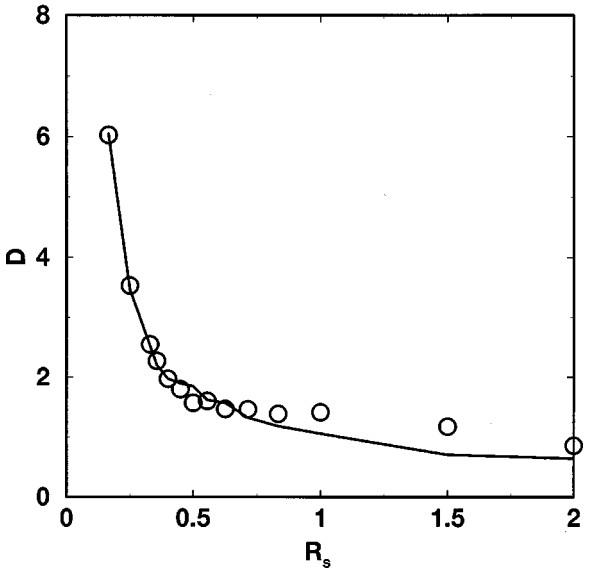

FIG. 9. Coefficient of diffusion for different values of R_s. $R_b=0.5$. ○: Numerical values obtained by simulation. Full line: theoretical values calculated from $v^2(\infty)/2\gamma$.

In Fig. 9, we compare, for different values of R_s, the diffusion coefficient found from the simulation with the theoretical value, $v^2(\infty)/2\gamma$, predicted by the Langevin equation combined with our analytical calculation of γ. The theoretical calculation of γ agrees very well with the simulation results. We recall that $1/\gamma$ corresponds to the characteristic time for the diffusive behavior. It is important to notice that γ can be approximated by ω_c only when $R_s \ll R_b$. Effectively, the calculation for $m_s \sim 0$ gives $\tilde{\nu}=-1$. Larger s particles need to suffer more than one collision to lose memory of their previous condition. For $m_s \sim \infty$, $\tilde{\nu}$ is found equal to zero. Using these methods, we find for the elastic monodisperse case ($R_s=R_b$) that relaxation (decorrelation) takes place after about three collisions.

The agreement between numerical results and theoretical predictions allows us to confirm our numerical algorithm.

IV. FORCED SYSTEM

In a real granular system dissipation occurs through collisions, a fact that must be taken into account. Experimental mechanical properties of grains (restitution and friction coefficients) and collision laws [12] are used in our simulations. The collisions between grains and the walls are treated with the same inelastic properties. Due to dissipation, we need to feed energy into the system to maintain the particles agitated. To accomplish this, we choose random heating [13,14]: At every time step δt we give a random acceleration, $\eta_i(t)$, in both spatial directions to each particle. The equation of motion can now be written formally as

$$m\frac{dv_i}{dt}=F_i^c+F_i^t, \qquad \langle F_i^t(t)F_j^t(t')\rangle = m^2\delta_{i,j}\delta(t-t')\,\eta_0^2. \tag{4.1}$$

F_i^c is the collision force acting on a particle of mass m. We chose the random acceleration, F_i^t/m, to be independent of the mass of the particle. It is given by a Gaussian noise of variance η_0^2.

At long time, the loss of energy due to collisions and the gain due to F^t balance each other such that the system reaches a steady state out of equilibrium. It can be shown [15] that the velocity distribution in this steady state is well described by a Maxwellian.

A. Stationary state

In the stationary state energy loss and gain balance exactly. The energy loss per unit time Γ for the s particle, can be expressed as

$$\Gamma = P(m_s,m_b)\,\omega_c m_s v^2, \tag{4.2}$$

where $P(m_s,m_b)$ is the relative energy loss of particle s due to collisions. Clearly as for $\tilde{\nu}$, Γ must depend on the mass of the particle and on the two velocities v_s and v_b. On the other hand, the gain of energy due the stochastic force is

$$\tfrac{1}{2}m_s[v^2(t+\delta t)-v^2(t)] = m_s\eta_0^2\delta t. \tag{4.3}$$

In the steady state of the monodisperse system [$R=R_s=R_b$, and $v^2(\infty)=$constant], we find, using Eq. (3.11), the following scaling for $v^2(\infty)$:

$$v^2(\infty)\propto(\eta_0^2)^{2/3}, \qquad v^2(\infty)\propto\tau_c. \tag{4.4}$$

We checked these two scaling laws numerically (see Fig. 10) and obtained the correct exponent 2/3 for the various coefficients of restitution used in the contact laws. We have also verified the predicted dependence on τ_c for different values

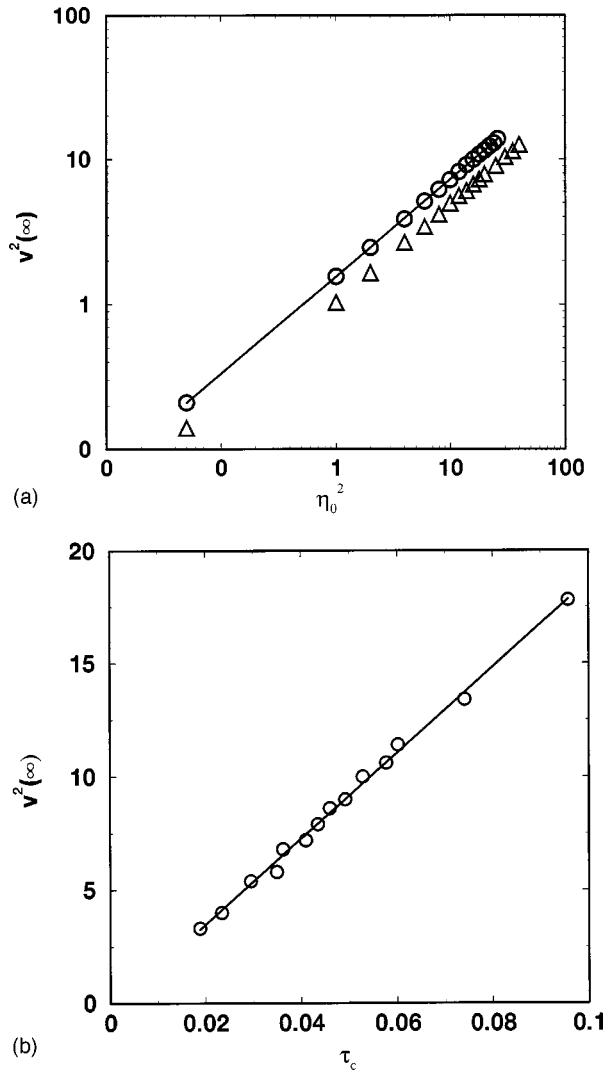

FIG. 10. (a) $v^2(\infty)$ vs η_0^2 for different coefficients of restitution. ○: $e_n=0.87$, $e_s=0.4$, $\mu=0.25$; △: $e_n=0.4$, $e_s=0.4$, $\mu=0.25$. (b) $v^2(\infty)$ vs the mean time between collisions τ_c.

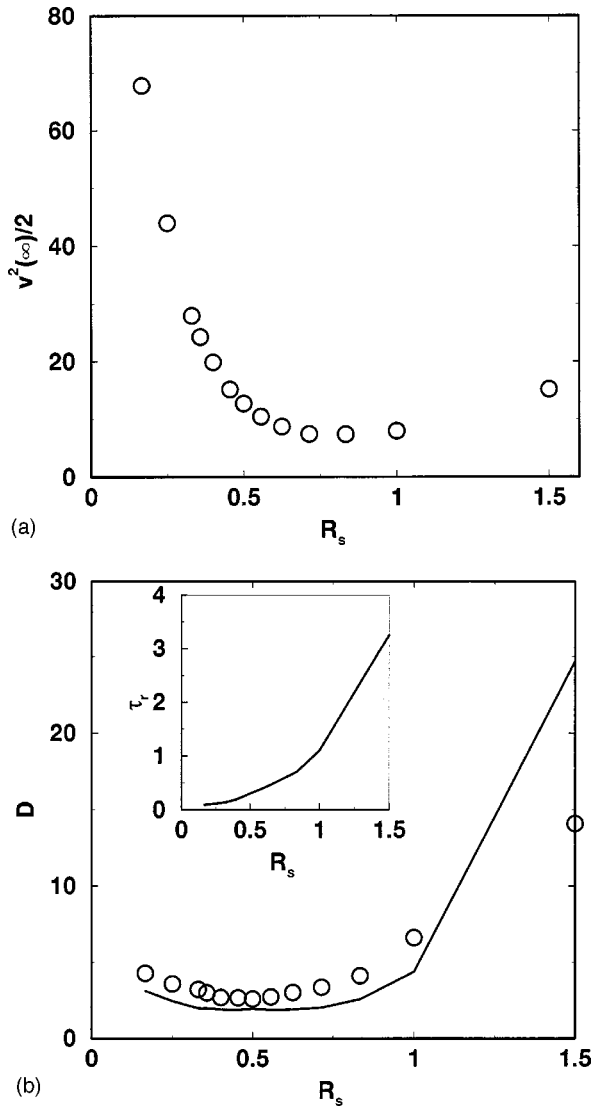

FIG. 11. (a) $v^2(\infty)$ vs R_s ($R_b=0.5$). (b) Coefficient of diffusion D as a function of R_s. ○: Numerical values obtained from simulation. Full line: corresponding values given by $v^2(\infty)/2\gamma$. The insert shows τ_r vs R_s.

of R. The good agreement between theory and simulation indicates that we can describe the system by macroscopic continuous equations if $\delta t \ll \tau_c$. As we explain elsewhere [16], the term $P(m,m)$ (in the monodisperse case) is independent of mass and velocity, because all particles are identical. This value of $P(m,m)$ was found equal approximately to 0.145 for the mechanical properties corresponding to acetate spheres [12]. We can then, in the case of a monodisperse system, predict the dependence of the mean-square velocity on the various parameters and, consequently, characterize the stationary state. For the bidisperse case, the calculation is more complicated. Indeed the loss of energy depends on the two types of colliding particles and also on the different coefficients of restitution and friction introduced in the collision laws. As we show [16] the dependence of $P(m_s,m_b)$ on v_s/v_b is not trivial.

In this paper we limit ourselves to the effect of the thermalization mode (or random force) on the diffusion coefficient. To this end, we will compare in the following section the simulation results for D with $v^2(\infty)/2\gamma$ from the Langevin equation.

B. Diffusion of one particle

To estimate D, we use reflecting boundaries and the same method explained in Sec. II B. We consider here the bidisperse case (a single particle of radius R_s in a sea of particles of radius R_b). As we have not yet found a theoretical expression for $P(m_s,m_b)$ for this case, we use for the mean-square velocities the values obtained from the simulations, which are shown in Fig. 11(a). Note that η_0^2 has been chosen such that the value of v_b^2 is the same as in the previous section. We see that $v^2(\infty)$ first decreases with R_s for $R_s<R_b$ but then increases when $R_s>R_b$. Because of dissipation and the random acceleration, the repartition of the energy with the mass is no longer proportional to $1/m_s$. In all cases it is possible to calculate the mean collision frequency for s with Eq. (3.11) and the associated γ value with Eq. (3.5). We can then calculate the relaxation time τ_r for all couples (R_s,R_b) used. In Fig. 11(b) we show the diffusion coefficient D, and

the relaxation time τ_r—in the inset—as functions of R_s. The behavior of $v^2(\infty)$ strongly modifies the curve of τ_r and D versus R_s compared to the elastic case. Note that the relaxation time represented in Fig. 11 clearly increases as R_s increases.

We have seen in the elastic case that $D=v^2/2\gamma$. In Fig. 11(b), we show the numerical results for D as a function of R_s and the corresponding values given by $v^2/2\gamma$. One can see clearly that the external noise modifies the dynamics of the granular gas and in particular the diffusion coefficient, D. The numerical value of D is found to be larger than that obtained by the corresponding random walk. Indeed, at short time, due to the random force, $v^2(t)$ is not constant. Between two collisions $v^2(t)$ increases linearly with t. Starting with the equation of motion of particle s (between two collisions),

$$\frac{dv_i(t)}{dt}=\eta_i(t), \tag{4.5}$$

and with the initial conditions $x_i(0)$ and $v_i(0)$, we can calculate mean-square displacement

$$\begin{aligned}&\langle[x_i(t)-x_i(0)]^2\rangle\\&\quad=\left\langle\int_{t_1=0}^{t}dt_1\left(v_i(0)+\int_0^{t_1}\eta_i(t_1')dt_1'\right)\right.\\&\qquad\left.\times\int_{t_2=0}^{t}dt_2\left(v_i(0)+\int_0^{t_2}\eta_i(t_2')dt_2'\right)\right\rangle.\end{aligned} \tag{4.6}$$

In two dimensions, this yields for the interval between two collisions

$$\langle[r(t)-r(0)]^2\rangle=v^2(0)t^2+\frac{2\eta_0^2}{3}t^3. \tag{4.7}$$

On the other hand, in the case of a random walk (or elastic collisions) the mean-square displacement at short time scales as t^2. This difference explains the disagreement between D and $v^2(\infty)/2\gamma$. As the velocity changes between two collisions the probability of collision is increasing with time too. The calculation of the coefficient of diffusion is not easy in this case, due to the correlation between the velocity and the probability of collision [see Eq. (3.11)]. For very small particles, if one approaches relaxation by the time of a new collision, i.e., $\tilde{\nu}\simeq -1$, this calculation should be possible. Indeed we can assume that the velocities before and after a collision are not correlated and have the same distribution (molecular chaos). We can then compute the mean-square displacement, knowing the dependence of the collision probability on the velocity [10]. With this assumption we improve the estimate of D for the smallest R_s. But for bigger particles we have seen that the velocities stay correlated over many collisions and we can no longer use molecular chaos.

V. CONCLUSIONS

We have presented here some general results about the diffusion process in an agitated granular gas. We first showed that the boundary conditions used in the simulations are of crucial importance. Indeed, periodic boundary conditions introduce artificially strong temporal correlations that alter the macroscopic properties of the gas. If we ensure that no correlations are induced by the algorithm, for example, by using reflecting boundaries, the numerical results obtained for an elastic gas can be described very well by a Langevin equation. We have presented a theoretical calculation of the relaxation time that allows us to predict the diffusion coefficient in all cases studied. This was not *a priori* intuitive since the radius of the particles is of the order of the mean-free-path. Finally we have analyzed the influence of uniform heating (a random acceleration) on dissipative gases. We have shown that heating influences the dynamics at short time. This is evident through the value of the diffusion coefficient, which is different from that expected from the Langevin description. We are now applying with success these results to the diffusion process in a granular mixture consisting of two type of grains (differing by mass or size) in equal proportion.

ACKNOWLEDGMENTS

This work was partially funded by the CNRS Programme International de Cooperation Scientifique PICS No. 753 and the Norwegian research council NFR.

[1] J. Schäfer, S. Dippel, and D. Wolf, J. Phys. I **6**, 5 (1996).
[2] M. P. Allen and D. J. Tildesley, *Computer Simulations of Liquids* (Oxford University Press, Oxford, 1987).
[3] J. M. Haile, *Molecular Dynamics Simulation, Elementary Methods* (Wiley-Interscience, New York, 1997).
[4] M. Ernst, H. Hauge, and J. M. J. van Leeuwen, Phys. Rev. A **4**, 2055 (1971).
[5] B. J. Alder and T. E. Wainwright, Phys. Rev. Lett. **18**, 988 (1967).
[6] B. J. Alder and T. E. Wainwright, Phys. Rev. A **1**, 18 (1970).
[7] I. Goldhirsh and G. Zanetti, Phys. Rev. Lett. **70**, 1619 (1993).
[8] I. Goldhirsh (private communication).
[9] C. Bizon, M. D. Shattuck, J. B. Swifft, and H. L. Swinney, Phys. Rev. E **60**, 4340 (1999).
[10] C. Henrique, Ph.D. thesis, Université de Rennes I, 1999.
[11] S. Chapmann and T. G. Cowling, *The Mathematical Theory of Nonuniform Gases* (Cambridge University Press, Cambridge, 1970).
[12] S. F. Foerster, M. Y. Louge, H. Chang, and K. Allia, Phys. Fluids **6**, 1108 (1994).
[13] T. P. C. van Noije, M. H. Ernst, E. Trizac, and I. Pagonarabarraga, Phys. Rev. E **59**, 4326 (1999).
[14] D. R. Williams and F. C. MacKintosh, Phys. Rev. E **54**, R9 (1996).
[15] G. Peng and T. Ohta, Phys. Rev. E **58**, 4737 (1998).
[16] C. Henrique, G. G. Batrouni, and D. Bideau, Phys. Rev. E (to be published).